PROGRESSIVE DAMAGE ANALYSIS OF COMPOSITE LAYERED PLATES USING A MESH REDUCTION METHOD

R. Zahari[1] and A. El-Zafrany[2]
[1] Department of Aerospace Engineering, Universiti Putra Malaysia, Serdang, 43400, Selangor, Malaysia.
[2] School of Engineering, Cranfield University, Cranfield, Bedford MK43 0AL, England.
Email: rizal@eng.upm.edu.my

ABSTRACT

A mesh reduced method (finite strip method), for non-linear stress analysis based on the tangential stiffness matrix has been developed using the new concept of polynomial finite strip elements, with Mindlin plate-bending theory for composite plates. A progressive damage methodology and algorithm for composite laminates was successfully developed for the new finite strip methods using stress-based failure criteria. A finite strip analysis programming package which is capable of performing non-linear progressive damage analysis for composite plates has also been developed with Mindlin plate bending element. Validation of the developed finite strip package has been successfully carried out by comparing the results with corresponding results obtained with the finite element analysis using ABAQUS and with some published experimental results. Good comparisons with the finite element results and experimental results were observed through various test cases, confirming the accuracy and reliability of the new derivations and the programming package.

Keywords: finite strip methods, Mindlin's plate bending theory, composite materials, progressive damage analysis.

INTRODUCTION

Thus far, many research on the progressive failure analysis of composite laminated plates and shells have been successfully carried out using the finite element method (FEM) in order to simulate failure modes in composite materials.. Although the finite element method is considered as a very powerful and versatile tool [1], it requires a sophisticated mesh generation for the analysis. The finite strip method (FSM) [2], which is a specialization of the FEM with a reduced dimensionality, can be used as an alternative to the FEM for the progressive damage analysis of composite laminates.

The failure analysis of composites which was performed by Lee [3] can be regarded as one of the first finite element based failure analysis. He performed a three-dimensional finite element analysis and employed his own direct-mode determining failure criterion to predict the failures in composite laminated plates subjected to uniaxial and biaxial loadings. Since then, there have been numerous literatures regarding the progressive failure analysis of composite laminated plates and shells [4 - 13], and stiffened panels using FEM, [14, 15].

The progressive damage analysis using finite strip methods (FSM) did not receive much attention so far. Cheung and Akhras [16] devised a finite strip method for the progressive failure analysis of composite laminates based on higher order shear deformation theory and Lee's failure criterion. The results of the finite strip method were in good agreement with existing analytical and numerical solutions. They also investigated the effects of fibre orientation and the number of plies on the load carrying capacity of composite laminates. However, only infinitesimal strain was considered in the formulation of the finite strip equations. Zhang et al. [17] developed a B-spline finite strip method to simulate large deflection and delamination behaviour of laminated composite plates subjected to transverse loading. In order to model progressive failure phenomena of composite laminates, both stress-based criteria and fracture mechanics-based criteria were employed, and the former for delamination whilst the later for delamination propagation. Good agreement between the finite strip method and the available experimental and analytical results has been achieved.

This paper presents the development of a progressive damage analysis methodology for stress analysis of composite layered plate using new derivations of finite strip methods. Non-linear equations will be derived using the tangential stiffness matrix approach, which is an improvement to the work of Razzaq [18, 19] with all integrations over the plate thickness carried out analytically. To the authors' conclusion, in the literature concerning the damage assessments of composites, very little work was reported which studied the non-linear damage progression in composite laminates using finite strip methods. Thus, it is one of the objectives of the author to develop the progressive damage analysis of composite laminates using finite strips equations.

DERIVATIONS OF FINITE STRIP EQUATIONS

In this work, the finite strip analysis of composite plates and shells, which is based on a new derivation of the first order shear element (*Mindlin type* element [20]) is presented taking into account the geometric non-linearity. This derivation follows concepts similar to those employed in the finite element analysis using the tangential stiffness matrix approach. The derivations are based on a new *Mindlin-type* finite strip element [18] and [19] in which one-dimensional *Lagrangian* interpolation will be employed along both the *x* and *y* directions together with appropriate reduced integration schemes.

Displacement and strain components

Consider a composite laminated plate which is parallel to the x-y plane. The upper and lower surfaces of the plate are defined by z = h/2 and z = - h/2 respectively, where h is the thickness of the plate Based on Reissner's theory [21], the transverse shear strains at any point (*x, y ,z*) inside a plate can be represented by parabolic distributions across the thickness of the plate as follows:

$$\underline{\gamma}(x, y, z) = \begin{bmatrix} \gamma_{xz} \\ \gamma_{yz} \end{bmatrix} = \frac{3}{2}\left[1 - \frac{4z^2}{h^2}\right]\begin{bmatrix} \bar{\gamma}_{xz} \\ \bar{\gamma}_{yz} \end{bmatrix} \tag{1}$$

where $\bar{\gamma}_{xz}$ and $\bar{\gamma}_{yz}$ are the average values of the transverse shear strains over plate thickness. The average values of the transverse shear can be used to define the displacement components, which leads to:

$$u(x,y,z) = u^{\mathrm{o}}(x,y) + z\,\theta_y(x,y) \tag{2}$$

$$v(x,y,z) = v^{\mathrm{o}}(x,y) - z\,\theta_x(x,y) \tag{3}$$

$$w(x,y,z) \cong w^{\mathrm{o}}(x,y) \tag{4}$$

Equations (2), (3), and (4) represent the displacement components at any point (*x, y, z*) inside the plate, $(\ )^{\mathrm{o}}$ are the values of *u, v* and *w* at the mid-plane of the plate ($z = 0$), and θ_x, θ_y represent average slope angles defined as follows:

$$\theta_x = +\left[\frac{\partial w}{\partial y} - \bar{\gamma}_{yz}\right] \tag{5}$$

$$\theta_y = -\left[\frac{\partial w}{\partial x} - \bar{\gamma}_{xz}\right] \tag{6}$$

In this work the transverse shear strains are always assumed infinitesimal while for non-linear static analysis, the x-y strain components are assumed finite. Using Green's strain displacement equations [22], the strain tensor at any point inside the plate can be obtained using appropriate engineering notations.

Interpolated Displacement Equations

Mindlin-type finite strip elements are based on employing piecewise one-dimensional Lagrangian interpolation along the x-direction in terms of n-node elements. On the other hand, a smooth polynomial of degree m-1 is employed along the width (y-direction) also using the Lagrangian interpolation. The full x-y interpolated displacement equations can be expressed for an n-node finite strip, with *m y*-terms (harmonics) as follows[18]:

$$u^{o}(x,y)=\sum_{i=1}^{n}\sum_{r=1}^{m}N_i(\xi)\mu_r(\eta)u_i^r \tag{7}$$

$$v^{o}(x,y)=\sum_{i=1}^{n}\sum_{r=1}^{m}N_i(\xi)\mu_r(\eta)v_i^r \tag{8}$$

$$w(x,y)=\sum_{i=1}^{n}\sum_{r=1}^{m}N_i(\xi)\mu_r(\eta)w_i^r \tag{9}$$

$$\theta_x(x,y)=\sum_{i=1}^{n}\sum_{r=1}^{m}N_i(\xi)\mu_r(\eta)(\theta_x^r)_i \tag{10}$$

$$\theta_y(x,y)=\sum_{i=1}^{n}\sum_{r=1}^{m}N_i(\xi)\mu_r(\eta)(\theta_y^r)_i \tag{11}$$

where the shape functions $N_{r(\zeta)}$ and $\mu_{r(\eta)}$ are

$$N_i(\xi)=\prod_{\substack{j=1\\ j\neq i}}^{n}\frac{(n-1)\xi-(j-1)}{i-j} \tag{12}$$

$$\mu_r(\eta)=\prod_{\substack{s=1\\ s\neq r}}^{m}\frac{(m-1)\eta-(s-1)}{r-s} \tag{13}$$

which represent one dimensional *Lagrangian* shape functions.

Interpolation of Strain Components

Transverse Shear Strains

From equations (9)-(11) it can be proved that:

$$\underline{\hat{\gamma}}(x,y)=\sum_{r=1}^{m}\sum_{i=1}^{n}\begin{bmatrix}\mu_r\dfrac{\partial N_i}{\partial x}w_i^r+N_i\mu_r(\theta_y^r)_i\\ \dfrac{\partial \mu_r}{\partial y}N_iw_i^r-N_i\mu_r(\theta_x^r)_i\end{bmatrix} \tag{14}$$

Notice that:

$$\frac{\partial N_i}{\partial x}=\frac{dN_i}{d\xi}\frac{d\xi}{dx}=\frac{1}{J_x}N_r'(\xi) \tag{15}$$

$$\frac{\partial \mu_r}{\partial y}=\frac{dN_i}{d\eta}\frac{d\eta}{dy}=\frac{1}{J_y}\mu_r'(\eta) \tag{16}$$

where

$$N_i^{'}(\xi) = \frac{dN_i}{d\xi}, \quad \mu_r^{'}(\eta) = \frac{d\mu_r}{d\eta} \tag{17}$$

Defining

$$\left(\underline{\delta}_b^r\right)^t = \left[w_1^r \ \left(\theta_x^r\right)_1 \ \left(\theta_y^r\right)_1 \cdots\cdots w_n^r \ \left(\theta_x^r\right)_n \ \left(\theta_y^r\right)_n \right] \tag{18}$$

then equation (14) can be rewritten in the following matrix form:

$$\underline{\hat{\gamma}}(x,y) = \sum_{r=1}^{m} \underline{B}_\gamma^r(x,y)\underline{\delta}_b^r \tag{19}$$

where

$$\underline{B}_\gamma^r = \begin{bmatrix} \cdots & \dfrac{N_i^{'}\mu_r}{J_x} & 0 & N_i\mu_r & \cdots \\ \cdots & \dfrac{N_i\mu_r^{'}}{J_y} & -N_i\mu_r & 0 & \cdots \end{bmatrix} \tag{20}$$

Notice also from equation (19) it can be deduced that:

$$\underline{\gamma}(x,y,z) = f_\gamma(z)\sum_{r=1}^{m} \underline{B}_\gamma^r(x,y)\underline{\delta}_b^r \tag{21}$$

Where

$$f_\gamma(z) = \frac{3}{2}\left(1 - \frac{4z^2}{h^2}\right) \tag{22}$$

The x-y Strain Components

The infinitesimal (small) strain components can be expressed by the following equation:

$$\underline{\varepsilon}_S = \underline{\varepsilon}_o - z\,\underline{\hat{\varepsilon}}_b \tag{23}$$

where

$$\underline{\varepsilon}_o(x,y) \equiv \sum_{r=1}^{m} \underline{B}_o^r(x,y)\underline{\delta}_o^r \tag{24}$$

with

$$\left(\underline{\delta}_o^r\right)^t = \left[u_1^r \ v_1^r \quad u_2^r \ v_2^r \ \cdots\cdots \ u_n^r \ \ v_n^r \right] \tag{25}$$

and

$$\underline{B}_o^r(x,y) = \begin{bmatrix} \cdots & \dfrac{N_i^{'}\mu_r}{J_x} & 0 & \cdots \\ \cdots & 0 & \dfrac{N_i\mu_r^{'}}{J_y} & \cdots \\ \cdots & \dfrac{N_i\mu_r^{'}}{J_y} & \dfrac{N_i^{'}\mu_r}{J_x} & \cdots \end{bmatrix} \tag{26}$$

Similarly it can be deduced that:

$$\underline{\hat{\varepsilon}}_b(x,y)=\sum_{r=1}^{m}\underline{B}_b^r(x,y)\underline{\delta}_b^r \tag{27}$$

where

$$\underline{B}_b^r(x,y)=\begin{bmatrix} \cdots & 0 & 0 & -\frac{N_i'\mu_r}{J_x} & \cdots \\ \cdots & 0 & \frac{N_i\mu_r'}{J_y} & 0 & \cdots \\ \cdots & 0 & \frac{N_i'\mu_r}{J_x} & -\frac{N_i\mu_r'}{J_y} & \cdots \end{bmatrix} \tag{28}$$

It can be proved that the rotation vectors [22]:

$$\underline{\theta}_m(x,y)=\begin{bmatrix} \frac{\partial u^o}{\partial x} \\ \frac{\partial v^o}{\partial x} \\ \frac{\partial u^o}{\partial y} \\ \frac{\partial v^o}{\partial y} \end{bmatrix}=\sum_{r=1}^{m}\sum_{i=1}^{n}\begin{bmatrix} \frac{N_i'}{J_x} & \mu_r & u_i^r \\ \frac{N_i'}{J_x} & \mu_r & v_i^r \\ N_i & \frac{\mu_r'}{J_y} & u_i^r \\ N_i & \frac{\mu_r'}{J_y} & v_i^r \end{bmatrix} \tag{29}$$

which can be rewritten as follows:

$$\underline{\theta}_m(x,y)=\sum_{r=1}^{m}\underline{G}_m^r(x,y)\underline{\delta}_o^r \tag{30}$$

where

$$\underline{G}_m^r(x,y)=\begin{bmatrix} \cdots & \frac{N_i'\mu_r}{J_x} & 0 & \cdots \\ \cdots & 0 & \frac{N_i'\mu_r}{J_x} & \cdots \\ \cdots & \frac{N_i\mu_r'}{J_y} & 0 & \cdots \\ \cdots & 0 & \frac{N_i\mu_r'}{J_y} & \cdots \end{bmatrix} \tag{31}$$

Similarly, it can be proved by using the same technique that:

$$\underline{\theta}_w(x,y)=\sum_{r=1}^{m}\underline{G}_w^r(x,y)\underline{\delta}_b^r \tag{32}$$

$$\underline{\theta}_{\theta}(x,y)=\sum_{r=1}^{m}\underline{G}_{\theta}^{r}(x,y)\underline{\delta}_{b}^{r} \tag{33}$$

where

$$\underline{G}_{w}^{r}(x,y)=\begin{bmatrix} \cdots & \frac{N_i'\mu_r}{J_x} & 0 & 0 & \cdots \\ \cdots & \frac{N_i'\mu_r}{J_y} & 0 & 0 & \cdots \end{bmatrix} \tag{34}$$

and

$$\underline{G}_{\theta}^{r}(x,y)=\begin{bmatrix} \cdots & 0 & 0 & -\frac{N_i'\mu_r}{J_x} & \cdots \\ \cdots & 0 & \frac{N_i'\mu_r}{J_x} & 0 & \cdots \\ \cdots & 0 & 0 & -\frac{N_i\mu_r'}{J_y} & \cdots \\ \cdots & 0 & \frac{N_i\mu_r'}{J_y} & 0 & \cdots \end{bmatrix} \tag{35}$$

Hence, it can also be proved that the total *x-y* strain (infinitesimal and large):

$$\underline{\varepsilon}(x,y,z)=\sum_{r=1}^{m}\left\{\left(\underline{B}_{o}^{r}\underline{\delta}_{o}^{r}+\frac{1}{2}\underline{B}_{mm}^{r}\ \underline{\delta}_{o}^{r}+\frac{1}{2}\underline{B}_{ww}^{r}\ \underline{\delta}_{b}^{r}\right)\right. \tag{36}$$

$$\left.-z\left(\underline{B}_{b}^{r}\underline{\delta}_{b}^{r}+\frac{1}{2}\underline{B}_{\theta m}^{r}\ \underline{\delta}_{o}^{r}+\frac{1}{2}\underline{B}_{m\theta}^{r}\ \underline{\delta}_{b}^{r}\right)+\frac{1}{2}z^{2}\underline{B}_{\theta\theta}^{r}\ \underline{\delta}_{b}^{r}\right\} \tag{37}$$

Where $\underline{B}_{mm}^{r},\underline{B}_{ww}^{r},\underline{B}_{m\theta}^{r},\underline{B}_{\theta m}^{r},\underline{B}_{\theta\theta}^{r}$ are the non-linear $\underline{B}$ matrices and are defined as follows:

$$\underline{B}_{ww}^{r}(x,y)=\underline{A}_{w}\underline{G}_{w}^{r} \tag{38}$$

$$\underline{B}_{pq}^{r}(x,y)=\underline{A}_{p}\underline{G}_{q}^{r} \tag{39}$$

where $p,q = m$ or θ

with all the $\underline{A}$ matrices defined as follows:

$$\underline{A}_{m}=\begin{bmatrix} \frac{\partial u^{o}}{\partial x} & \frac{\partial v^{o}}{\partial x} & 0 & 0 \\ 0 & 0 & \frac{\partial u^{o}}{\partial y} & \frac{\partial v^{o}}{\partial y} \\ \frac{\partial u^{o}}{\partial y} & \frac{\partial v^{o}}{\partial y} & \frac{\partial u^{o}}{\partial x} & \frac{\partial v^{o}}{\partial x} \end{bmatrix} \tag{40}$$

$$\underline{A}_w = \begin{bmatrix} \frac{\partial w}{\partial x} & 0 \\ 0 & \frac{\partial w}{\partial y} \\ \frac{\partial w}{\partial y} & \frac{\partial w}{\partial x} \end{bmatrix} \tag{41}$$

$$\underline{A}_\theta = \begin{bmatrix} \left(-\frac{\partial \theta_y}{\partial x}\right) & \frac{\partial \theta_x}{\partial x} & 0 & 0 \\ 0 & 0 & \left(-\frac{\partial \theta_y}{\partial y}\right) & \frac{\partial \theta_x}{\partial y} \\ \left(-\frac{\partial \theta_y}{\partial y}\right) & \frac{\partial \theta_x}{\partial y} & \left(-\frac{\partial \theta_y}{\partial x}\right) & \frac{\partial \theta_x}{\partial x} \end{bmatrix} \tag{42}$$

Stress Components

The stress components at a point in the l^{th} layer, can also be partitioned and represented by the following vectors [22]:

$$\underline{\sigma}^{(l)} = \begin{bmatrix} \sigma_x \\ \sigma_y \\ \tau_{xy} \end{bmatrix} \tag{43}$$

$$\underline{\tau}^{(l)} = \begin{bmatrix} \tau_{xz} \\ \tau_{yz} \end{bmatrix} \tag{44}$$

Using stress-strain relations for the l^{th} layer, then:

$$\underline{\sigma}^{(l)} = \underline{D}^{(l)} \underline{\varepsilon} \tag{45}$$

$$\underline{\tau}^{(l)} = \underline{\mu}^{(l)} \underline{\gamma} \tag{46}$$

where $\underline{D}^{(l)}, \underline{\mu}^{(l)}$ are material stiffness matrices with respect to plate axes, for the l^{th} layer.

Derivation of element stiffness matrices

Using the principle of virtual work, the work done by actual loads is equal to the work done by equivalent nodal loading [22], i.e.:

$$d\chi = dU - dW = 0 \tag{47}$$

We then arrived at the following tangential stiffness matrix terms which are defined for one strip:

$$\begin{aligned} \underline{K}_{oo}^{sr} = \iint_{strip} \Big\{ & \left(\underline{B}_o^s + \underline{B}_{mm}^s\right)^t \left[\underline{D}_{(0)}\left(\underline{B}_o^r + \underline{B}_{mm}^r\right) - \underline{D}_{(1)}\underline{B}_{\theta m}^r\right] \\ & + \left(\underline{B}_{\theta m}^s\right)^t \left[\underline{D}_{(2)}\underline{B}_{\theta m}^r - \underline{D}_{(1)}\left(\underline{B}_o^r + \underline{B}_{mm}^r\right)\right]\Big\}\, dx\, dy \end{aligned} \tag{48}$$

$$\underline{K}_{ob}^{sr} = \iint_{strip} \left\{ \left(\underline{B}_o^s + \underline{B}_{mm}^s\right)^t \left[\underline{D}_{(0)}\underline{B}_{ww}^r - \underline{D}_{(1)}\left(\underline{B}_b^r + \underline{B}_{m\theta}^r\right) + \underline{D}_{(2)}\underline{B}_{\theta\theta}^r\right]\right.$$

$$\left. + \left(\underline{B}_{\theta m}^s\right)^t \left[-\underline{D}_{(1)}\underline{B}_{ww}^r + \underline{D}_{(2)}\left(\underline{B}_b^r + \underline{B}_{m\theta}^r\right) - \underline{D}_{(3)}\underline{B}_{\theta\theta}^r\right]\right\} dx\,dy \qquad (49)$$

$$\underline{K}_{bo}^{sr} = \iint_{strip} \left\{ \left(\underline{B}_{ww}^s\right)^t \left[\underline{D}_{(0)}\left(\underline{B}_o^r + \underline{B}_{mm}^r\right) - \underline{D}_{(1)}\underline{B}_{\theta m}^r\right] + \left(\underline{B}_b^s + \underline{B}_{m\theta}^s\right)^t \left[-\underline{D}_{(1)}\left(\underline{B}_o^r + \underline{B}_{mm}^r\right) + \underline{D}_{(2)}\underline{B}_{\theta m}^r\right.\right.$$

$$\left.\left. + \left(\underline{B}_{\theta\theta}^s\right)^t \left[\underline{D}_{(2)}\left(\underline{B}_o^r + \underline{B}_{mm}^r\right) - \underline{D}_{(3)}\underline{B}_{\theta m}^r\right]\right\} dx\,dy \qquad (50)$$

$$\underline{K}_{\gamma\gamma}^{sr} = \iint_{strip} \left(\underline{B}_\gamma^s\right)^t \underline{\mu}_{\gamma\gamma}\, \underline{B}_\gamma^r \, dx\,dy \qquad (51)$$

$$\underline{K}_{bb}^{sr} = \iint_{strip} \left\{ \left(\underline{B}_{ww}^s\right)^t \left[\underline{D}_{(0)}\underline{B}_{ww}^r - \underline{D}_{(1)}\left(\underline{B}_b^r + \underline{B}_{m\theta}^r\right) + \underline{D}_{(2)}\underline{B}_{\theta\theta}^r\right] + \left(\underline{B}_b^s + \underline{B}_{m\theta}^s\right)^t \left[-\underline{D}_{(1)}\underline{B}_{ww}^r\right.\right.$$

$$\left.\left. + \underline{D}_{(2)}\left(\underline{B}_b^r + \underline{B}_{m\theta}^r\right) - \underline{D}_{(3)}\underline{B}_{\theta\theta}^r\right] + \left(\underline{B}_{\theta\theta}^s\right)^t \left[\underline{D}_{(2)}\underline{B}_{ww}^r - \underline{D}_{(3)}\left(\underline{B}_b^r + \underline{B}_{m\theta}^r\right) + \underline{D}_{(4)}\underline{B}_{\theta\theta}^r\right]\right\} dx\,dy \qquad (52)$$

where

$$\underline{D}_{(n)} = \int_{-h/2}^{h/2} z^n\, \underline{D}^{(l)}\, dz \qquad (53)$$

represents the integrated material stiffness matrix integrated across the thickness of plate [22].

The following non-linear stiffness matrix terms can be defined for a strip:

$$\underline{K}_{mm}^{sr} = \iint_{strip} \left(\underline{G}_m^s\right)^t \underline{S}_{(0)}\, \underline{G}_m^r \, dx\,dy \qquad (54)$$

$$\underline{K}_{m\theta}^{sr} = \iint_{strip} \left(\underline{G}_m^s\right)^t \underline{S}_{(1)}\, \underline{G}_\theta^r \, dx\,dy \qquad (55)$$

$$\underline{K}_{\theta m}^{sr} = \iint_{strip} \left(\underline{G}_\theta^s\right)^t \underline{S}_{(1)}\, \underline{G}_m^r \, dx\,dy \qquad (56)$$

$$\underline{K}_{ww}^{sr} = \iint_{strip} \left(\underline{G}_w^s\right)^t \underline{S}_w\, \underline{G}_w^r \, dx\,dy \qquad (57)$$

$$\underline{K}_{\theta\theta}^{sr} = \iint_{strip} \left(\underline{G}_\theta^s\right)^t \underline{S}_{(2)}\, \underline{G}_\theta^r \, dx\,dy \qquad (58)$$

Where $\underline{S}$ represents the stress matrices integrated over the thickness [22]

Matrix Form of Linearized Equations

The non-linear static analysis can be linearized and be written in the following matrix form:

$$\sum_{strip} \left(\underline{K} + \underline{K}_\sigma\right) d\underline{\delta} = \underline{R} \qquad (59)$$

where $\underline{K}$ and $\underline{K}_\sigma$ are the tangential and non-linear stiffness matrices respectively. The residual force and nodal displacement vectors $\underline{R}$ and $\underline{\delta}$ respectively are defined as follows

$$d\underline{\delta}^t = \left[d\underline{\delta}^1 \quad d\underline{\delta}^2 \cdots d\underline{\delta}^r \cdots d\underline{\delta}^m\right] \qquad (60)$$

$$\underline{R}^t = \left[\underline{R}^1 \quad \underline{R}^2 \cdots \underline{R}^s \cdots \underline{R}^m\right] \qquad (61)$$

If $d\underline{\delta}^r$, $\underline{R}^s$ are defined such that:

$$\left(d\underline{\delta}^r\right) = \begin{bmatrix} d\underline{\delta}_o^r \\ d\underline{\delta}_b^r \end{bmatrix} \tag{62}$$

$$\underline{R}^s = \begin{bmatrix} \underline{R}_o^s \\ \underline{R}_b^s \end{bmatrix} \tag{63}$$

Where

$$\underline{R}_o^s = \sum_{strip} \sum_{r=1}^{m} \left\{ \left[\underline{K}_{oo}^{sr} d\underline{\delta}_o^r + \underline{K}_{ob}^{sr} d\underline{\delta}_b^r \right] + \left[\underline{K}_{mm}^{sr} d\underline{\delta}_o^r + \underline{K}_{m\theta}^{sr} d\underline{\delta}_b^r \right] \right\} \tag{64}$$

$$\underline{R}_b^s = \sum_{strip} \sum_{r=1}^{m} \left\{ \left[\underline{K}_{bo}^{sr} d\underline{\delta}_o^r + \left(\underline{K}_{\gamma\gamma}^{sr} + \underline{K}_{bb}^{sr} \right) d\underline{\delta}_b^r \right] + \left[\underline{K}_{\theta m}^{sr} d\underline{\delta}_o^r + \left(\underline{K}_{ww}^{sr} + \underline{K}_{\theta\theta}^{sr} \right) d\underline{\delta}_b^r \right] \right\} \tag{65}$$

for s = 1, 2,3, ….. , m.

Therefore, the partitioned element matrices can be defined as follows:

$$\underline{K}^{sr} = \begin{bmatrix} \underline{K}_{oo}^{sr} & \underline{K}_{ob}^{sr} \\ \underline{K}_{bo}^{sr} & \left(\underline{K}_{\gamma\gamma}^{sr} + \underline{K}_{bb}^{sr} \right) \end{bmatrix} \tag{66}$$

$$\underline{K}_{\sigma}^{sr} = \begin{bmatrix} \underline{K}_{mm}^{sr} & \underline{K}_{m\theta}^{sr} \\ \underline{K}_{\theta m}^{sr} & \left(\underline{K}_{ww}^{sr} + \underline{K}_{\theta\theta}^{sr} \right) \end{bmatrix} \tag{67}$$

PROGRESSIVE DAMAGE METHODOLOGY

A progressive failure methodology is developed for predicting the failure of laminate composite plates and shells under geometrically non-linear deformations. Using *Mindlin*-type, element. The failure criteria included in the present failure assessment are the stress-based failure criteria proposed by Tsai-Hill [23], Hoffman [24] and Tsai-Wu [25]. An algorithm for a progressive failure analysis has been developed and is illustrated in Figure 1. The analysis begins with the description of the finite strip model such as the boundary and loading conditions, and material properties. The second step is to compute the stiffness matrices for each strip and to assemble them to form global stiffness matrix. Next, nodal stresses at each ply, each node, each y value and each z-point are calculated and transformed into the material axes. The values of the transformed nodal stresses at the middle layer of each ply at each y value are used with one of the failure criteria to determine whether any failures have occurred at each load increment. If failures are detected, i.e. if the transformed stresses exceeded the respective failure criteria, a reduction in the value of the material properties will take place using a material degradation model which will be discussed in the next section. Equilibrium will then be re-established by evaluating the residual vector by using equation (63). If convergence is achieved after establishing equilibrium, then the applied load or displacement is increased. On the other hand, if a converged solution is not attained, the non-linear analysis at the same load increment will be repeated until a converged solution is found. The process is repeated until the catastrophic failure of the structure is reached.

Damage Modelling

In this research, a material degradation model based upon a total element or strip reduction method is implemented [26]. For each node at any y value of each ply (middle surface) that fails, the particular strip is reduced using a stiffness reduction factor given by the following equation:

$$\text{Stiffness Reduction Factor}(SRF) = 1.0 - \frac{\text{No. of Occurrence of Failure}}{\left(\text{No. of Nodes} \times \text{No. of } y \text{ terms}\right)} \tag{68}$$

For a two-noded strip which consists of two *y* terms, the overall stiffness of that particular strip is reduced by 25% if one of the nodes at one of the y terms has failed. Likewise, the stiffness reduction continues to occur as more points in a particular strip fail. If all the points in a particular strip satisfy the respective failure criterion, then the strip is assumed to have failed completely and the value of the stiffness reduction factor (*SRF*) equals zero. This adjustment accounts for the material non-linearity associated with a progressive failure analysis included within a non-linear finite strip analysis.

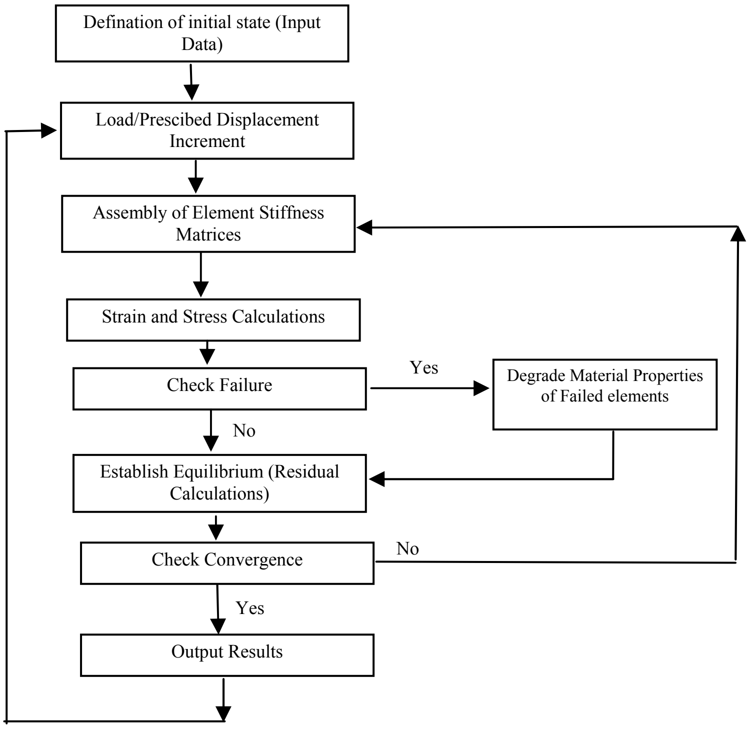

Figure 1: Progressive failure analysis algorithm

NUMERICAL EXAMPLES

A finite strip programming package has been developed based on the new derivations of finite strip methods. In order to validate the new finite strip methods and to test the capability of the newly developed package, a number of validation procedures using different case studies will be presented. The validation has been performed by comparing the results of the progressive damage analysis with corresponding results from a commercial finite element solver package.

In the validation procedure, the commercial package PATRAN has been used as a pre- and post-processor for generating finite element models and for displaying contour plots. The commercial package ABAQUS [27] has been used as the solver in the finite element analysis. All the progressive damage analyses using ABAQUS have been achieved by linking the non-linear analysis with a user-written subroutine (USLFLD) [27]. The user subroutine is written in FORTRAN language where it is saved as an independent file which contains the equation of one of the stress based failure theories. On the other hand, the finite strip meshes have been generated by a built-in one-dimensional mesh generator, which are much simpler to create than the commercial package finite element meshes.

Progressive Damage Analysis of Cantilever Plate

The analysis of cantilever plate with different types of loading has been carried out in order to assess the accuracy of the progressive damage methodology. Three types of load cases were considered namely:

1) **Tensile load** in terms of a uniform line tensile force.
2) **In-plane bending**, induced by a uniform in-plane shear force.
3) **Out-of-plane bending**, induced by a uniform out-of-plane line shear force.

Each type of load case including the geometry and boundary conditions is shown schematically in Figure 2.

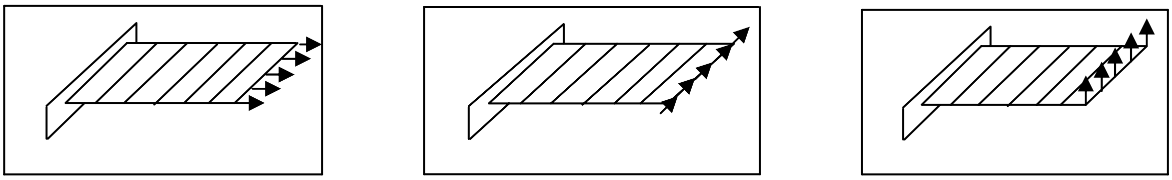

(a) Tension (b) In-plane-bending (c) Out-of-plane-bending

Figure 2: Schematic drawing showing the finite strip mesh of cantilever plate under various loading conditions.

The results of each case study were validated against ABAQUS. Tsai-Wu criterion was used for the failure criteria in this validation. A 12-ply cantilever plate made of Carbon/Epoxy with stacking sequence of $[-45/0/45]_{2s}$ has been considered in this case. The thickness of each ply, the stacking sequence and the lamina material properties for the laminate are given as

$$E_{11} = 134.75 \text{ GPa} \quad E_{22} = 8.24 \text{ GPa}, \; G_{12} = G_{23} = G_{31} = 7.0 \text{ GPa}, \; \nu_{12} = 0.325,$$

Thickness of each layer = 0.0025 m

$$X_t = 1500.0 \text{ MPa}, \; X_c = 1200.0 \text{ MPa}, \; Y_t = 50.0 \text{ MPa}, \; Y_c = 250.0 \text{ MPa}, \; S = 70.0 \text{MPa}$$

The type of element used for ABAQUS is the 4-noded quadrilateral with full in-plane integration points called, S4. For the purpose of validation, it is sufficient to use six 3-noded finite strip elements in the finite strip meshes after performing a mesh convergence study.

Cantilever Plate under Tension

A non-linear static analysis has been carried out for the cantilever plate under tension, A line force of intensity 2.0×10^6 N/m was applied axially (x-direction). The analysis was carried out for *Mindlin*-type element and its structural response before and after failure assessments were compared with ABAQUS using the S4 element.

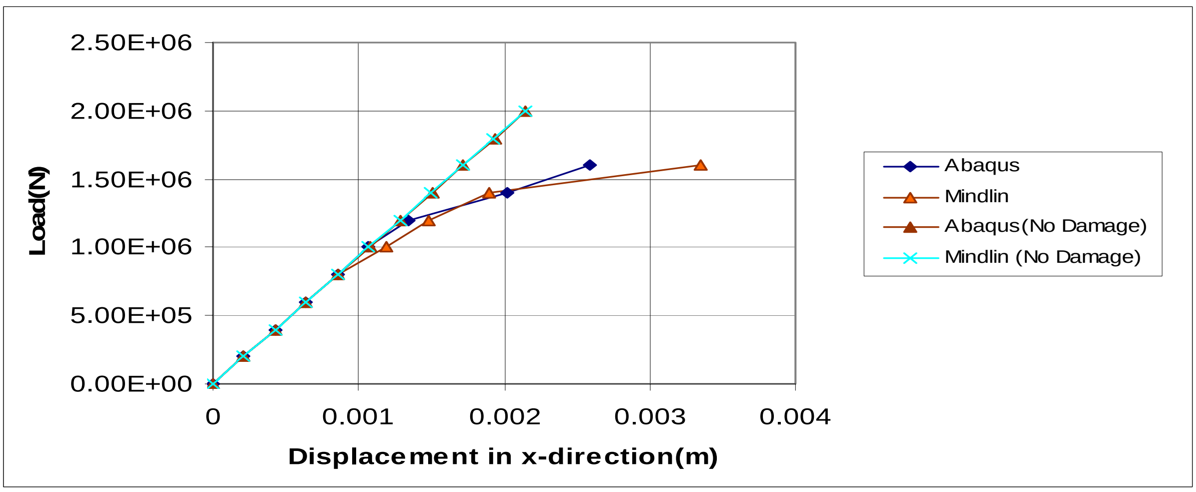

Figure 3: Cantilever plate under tension

Load-deflection curves were obtained which compare the finite strip results using *Mindlin*-type element with ABAQUS finite element results. The displacements were measured at the free end of the plate. By referring to figure 3, all the non-linear static analysis (without damage assessment) results agree very well with ABAQUS finite element results. From the figure, it can be seen that all the progressive failure results agree reasonably well with the results from ABAQUS although there is slight difference between them in the upper region of the curves. This may be due to the use of slightly different implementations of damage modeling between the finite strip and finite element.

Cantilever Plate under In-plane-Bending

A non-linear static analysis has been carried out for the cantilever plate under in-plane-bending. A line shear force of intensity 1.3×10^5 N/m was applied in y-direction. The analysis was carried out for *Mindlin*-type element and their structural response with damage assessments were compared with that from ABAQUS. Load-deflection curves were obtained which compares the finite strip results using *Mindlin*-type element with ABAQUS finite element results. The displacements were measured at the free end of the plate. By referring to figure 4, it can be noticed that all the progressive failure results from finite strip agree reasonably well with the results from ABAQUS.

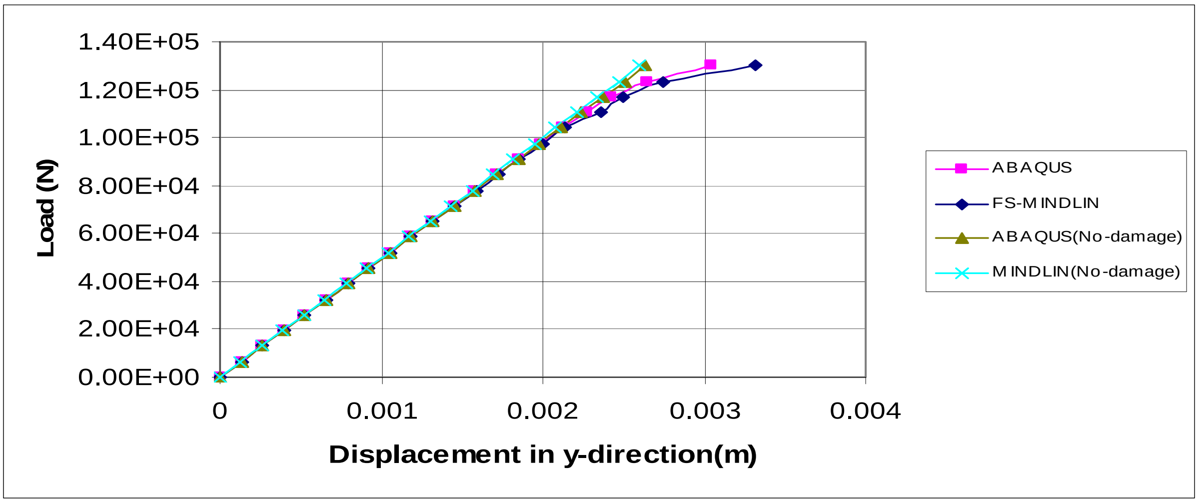

Figure 4: Cantilever plate under in-plane bending

Cantilever Plate under Out-of-Plane-Bending

A non-linear static analysis has been carried out for the cantilever plate under out-of-plane-bending. A line out-of-plane force of intensity 8.0×10^3 N/m was applied in *z*-direction. Progressive damage analysis was carried out for *Mindlin*-type, and its structural response was compared with that from ABAQUS. Load-deflection curves were obtained which compares the finite strip using *Mindlin*-type element with ABAQUS finite element results for both with and without damage assessments. By referring to figure 5 it can be noticed that all the progressive failure results from finite strip agree reasonably well with the results from ABAQUS. On the other hand, the non-linear static analysis results without damage consideration were also very good. Again, from the figure it can be seen that there is a slight discrepancies in the non-linear region of the curves which may due to the use of a slightly different implementations of damage modeling between the finite strip and the finite element.

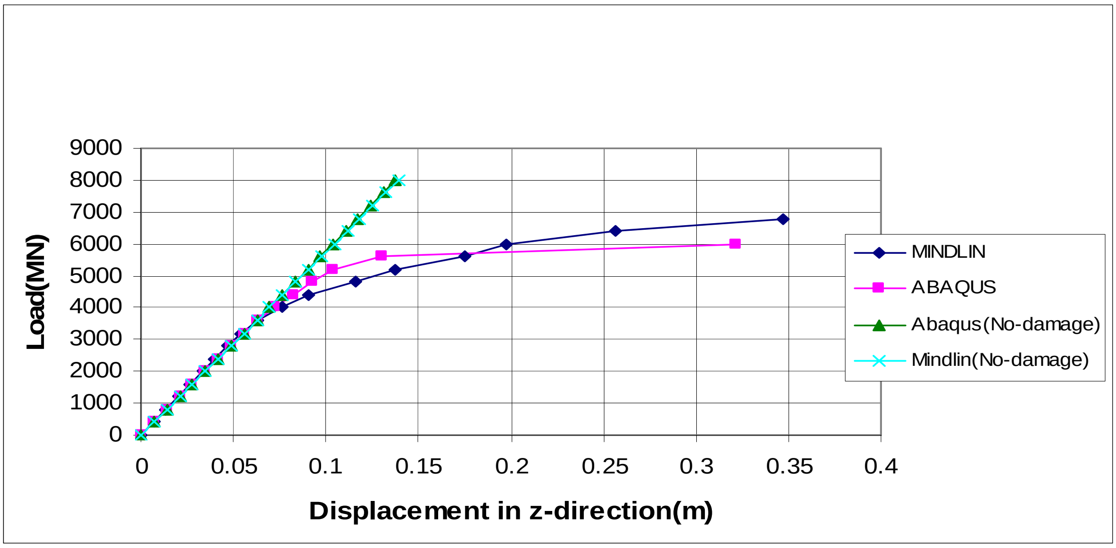

Figure 5: Cantilever plate under out-of-plane bending

Progressive damage analysis of Rectangular plate

A two-layer Carbon-Epoxy rectangular plate, with antisymmetric cross ply [0/90], simply supported at two sides only under uniformly distributed transverse load has been analyzed in this case (see figure 6). The load and boundary conditions of the rectangular plate including its dimensions and material properties are similar to those used by Reddy [28] as follows:

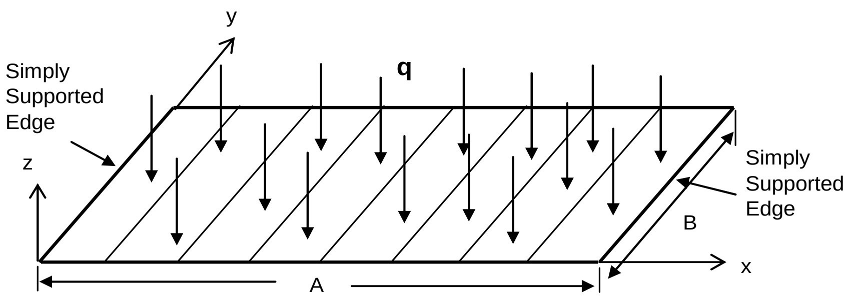

Figure 6: Schematic drawing of the rectangular plate subjected to uniform pressure,q.

A=1.5 in, B = 9.0in, Thickness of plate, h =0.04 in

E_{11}=20 msi, E_{22} = 1.4 msi, $G_{12} = G_{13} = G_{23}$ = 0.7 msi,

X_t = 309.0 ksi, X_c =159.0 ksi, Y_t=11.6 ksi, Y_c = 29.0 ksi, S = 23.2 ksi

For this test case 12 finite strip elements (Mindlin-type) were used to model the rectangular plate. The results of the maximum non-dimensional central deflection under uniformly distributed transverse loads are given in Table 1, and the results obtained using finite elements [28] and finite strips [17] are also recorded in the same table as comparison. It is interesting to see that the results of the present finite strip analysis are in excellent agreement with the results obtained by both researchers mentioned above.

Table 1: Non-dimensional out-of-plane central deflections of rectangular plate under uniformly distributed loads.

Load q (psi)	Non-dimensional out-of-plane deflections, w/h		
	Present FS method *(Mindlin)*	Zhang et al [17]	Reddy,[28]
0.04	-1.037	-1.035	-1.034
0.05	-1.100	-1.100	-1.100
0.10	-1.330	-1.328	-1.327
0.25	-1.710	-1.705	-1.705
0.50	-2.077	-2.073	-2.075
0.75	-2.330	-2.330	-2.332
1.00	-2.540	-2.535	-2.532

Progressive Damage Analysis of Square Plate

The accuracy of the present finite strip methods is further demonstrated considering a square plate under a uniform distributed load. In this case, a four-layer [0/90/90/0] square cross-ply laminated plate subjected to a uniform distributed transverse loading has been considered. The plate is assumed to be clamped along all four edges and is subjected to a uniform load intensity of 13.8 kPa. The laminate material properties and dimensions are as follows

$E_{11} = E_{22} = 12.61$ GPa, $G_{12} = G_{23} = G_{31} = 2.15$ GPa, $v_{12} = 0.24$,

length and width of plate = 304.8 mm, thickness of each layer = 0.6 mm,

$X_t = 1316.94$ MPa, $X_c = 1220.0$ MPa, $Y_t = 42.75$ MPa, $Y_c = 168.20$, $S = 48.30$ MPa

Non-linear progressive damage analysis has been performed using the present finite strip analysis (Mindlin element) and the results were compared with the results from ABAQUS and existing experimental results [29]. In figure 7, the centre deflection of the square plate under uniform distributed load was presented. From the figure, the finite strip results obtained using Mindlin element are in better agreement with the experimental results than those obtained using the ABAQUS finite element analysis. The maximum difference in the results between the finite strip analyses and the experimental is only about 10 percent. In contrast, 17 percent difference in the results has been observed between ABAQUS and the experimental results. The difference may be attributed to the inaccurate modelling of the clamped experimental boundary conditions, which may result in a small deviation on the deflections of the laminate.

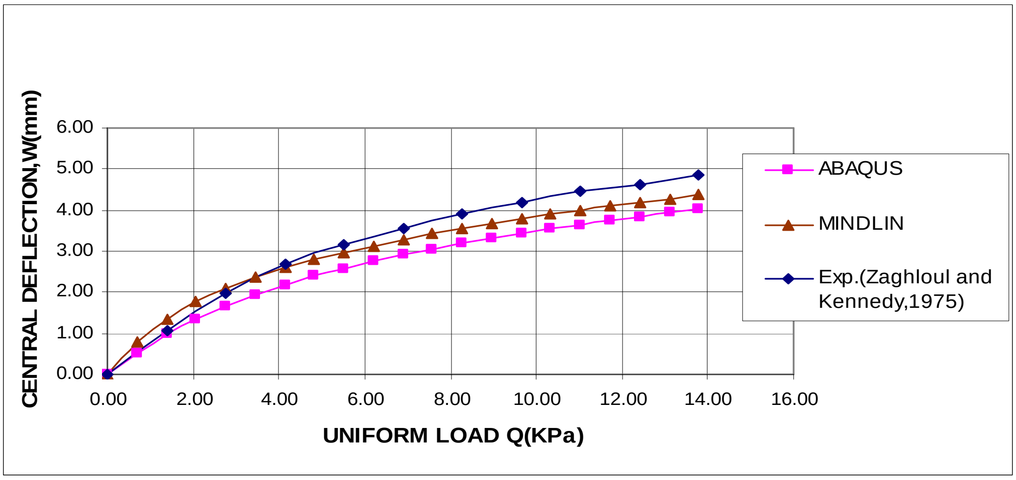

Figure 7: Square plate under uniform pressure

CONCLUSIONS

The work presented in this research contributes to the development of finite strip methods capable of simulating the damage or failure of composite laminates via a non-linear progressive damage analysis. Validation of the developed finite strip package has been successfully carried out by comparing the results with the finite element analysis using ABAQUS and with some published experimental results. A significant reduction in the modelling and effort as a result of only one-dimensional mesh required to model plates by using the package built-in mesh generator. Good comparison with the finite element results (ABAQUS) and experimental results were observed from previous test cases, confirming the accuracy and reliability of the new derivations, damage algorithm and the programming package.

REFERENCES

[1] Zienkiewicz, O.C. & Taylor, R.L. (2000) The finite element method. 5th edition, Butterworth & Heinemann, Oxford.
[2] Cheung, Y.K. (1976) Finite strip method in structural analysis. Oxford: Pergamon Press.
[3] Lee, J.D. (1982) Three dimensional finite element analysis of damage accumulation in composite laminate. Computers & Structures **15**: 335-350.
[4] Chang, F.K. & Chang, K.Y. (1987) A progressive damage model for laminated composites containing stress concentrations. Journal of Composite Materials **21**: 834-855.
[5] Chang, F.K. & Lessard, L.B. (1991) Damage tolerance of laminated composites containing an open hole and subjected to compressive loadings: Part I. Analysis. Journal of Composite Materials **25**: 2-43.
[6] Padhi, G.S., Shenoi, R.A., Moy, S.S.J. & Hawkins, G.L. (1998) Progressive failure and ultimate collapse of laminated composite plates in bending. Composite Structures **40**: 277-291.
[7] Reddy, Y.S.N., Moorthy, C.M.D & Reddy, J.N. (1995) Non-linear progressive failure analysis of laminated composite plates. Int. J. Non-Linear Mechanics **30**: 629-649.
[8] Tan, S.C. A progressive failure model for composite laminates containing openings. (1991) Journal of Composite Materials **25**: 556-77.
[9] Kim, Y., Davalos, J.F. & Barbero, E.J. (1996) Progressive failure analysis of laminated composite beams. Journal of Composite Materials **30**: 536.
[10] Gummadi, L.N.B. & Palazotto, A.N. (1998) Progressive failure analysis of composite cylindrical shells considering large rotations. Composite Part B **29B**: 547-563.
[11] Singh, S.B. & Kumar, A. (1999) Postbuckling response and strength of laminates under combined in-plane loads. Composites Science & Technology **59**: 727-736.
[12] Goyal, V.K., Jaunky, N.R., Johnson, E.R. & Ambur, D.R. (2004) Intralaminar and interlaminar progressive failure analyses of composite panels with circular cutouts. Composite Structures **64**: 91-105.
[13] Ambur, D.R., Jaunky, N., Hilburger, M.W. & Davila, C.G. (2004) Progressive failure analyses of compression-loaded composite curved panels with and without cutouts. Composite Structures **65**: 143-155.
[14] Sleight, D.W. (1999) Progressive failure analysis methodology for laminated composite structures. NASA/TP-1999-209107.
[15] Ambur, D.R., Jaunky, N. & Hilburger, M.W. (2004) Progressive failure studies of stiffened panels subjected to shear loading. Composite Structures **65**: 129-142.
[16] Cheung, M.S., Akhras, G. & Li, W. (1995) Progressive failure analysis of composite plates by the finite strip method. Computer Methods in Applied Mechanics & Engineering **124**: 49-61.
[17] Zhang, Y., Wang, S. & Petersson, B. (2003) Large deflection analysis of composite laminates. Journal of Materials Processing Technology **138**: 34-40.
[18] Razzaq, RJ. El-Zafrany, A. (2004) A mesh reduction method for the stress analysis of composite plates and shells. In Brebia, CA, editor. Boundary elements XXVI. Southampton, England: WIT Press.
[19] Razzaq, R.J. (2003) Nonlinear static and dynamic analysis of composite layered plates and shells using finite strip methods. PhD Thesis. Cranfield University.
[20] Mindlin, R.D. (1951) Influence of rotary inertia and shear in flexural motions of isotropic elastic plates. Journal of Applied Mechanics **18**: 31-38.
[21] Reissner, E. (1945) The effect of transverse shear deformation on the bending of elastic plates. Journal of Applied Mechanics **12**: 69-76.
[22] Rizal, Z. (2005) Progressive damage analysis of composite layered plates and shells using finite strip methods. PhD Thesis. Cranfield University.

[23] Hill, R. (1948) A theory of the yielding and plastic flow of anisotropic metals. Proceedings of the Royal Society of London, Series A **193**: 281-297.
[24] Hoffman, O. (1967) The brittle strength of orthotropic materials. Journal of Composite Materials, **1**: 200-206.
[25] Tsai, S.W. & Wu, E.M. (1971) A general theory of strength for anisotropic materials. Journal of Composite Materials, **5**: 58-80.
[26] Spottswood, S.M. & Palazotto, A.N. (2001) Progressive failure analysis of a composite shell. Composite Structures **53**: 117-131.
[27] ABAQUS. (2003) ABAQUS User's manual, Vol. 1-3, Version 6.4. Pawtucket, RI:Hibbitt, Karlsson & Sorensen.
[28] Reddy, J.N. (1989) On refined computational models of composite laminates. Int. J. Numer. Methods Engng. **27**: 361-382.
[29] Zaghloul, S.A. & Kennedy, J.B. (1975) Nonlinear behaviour of symmetrically laminated plates. Journal of Applied Mechanics **42**: 234-236.